ELEVENTH INTERNATIONAL CONFERENCE ON INTERGRANULAR AND INTERPHASE BOUNDARIES 2004

JOURNAL OF MATERIALS SCIENCE **40** (2005) 3115–3119

Brownian motion of liquid lead inclusions along dislocations in aluminum

E. JOHNSON*
Nano Science Center, Niels Bohr Institute, University of Copenhagen, Denmark; Department of Materials Research, Risø, Roskilde, Denmark
E-mail: johnson@fys.ku.dk

S. STEENSTRUP, M. LEVINSEN
Niels Bohr Institute, University of Copenhagen, Denmark

V. PROKOFJEV, V. ZHILIN
Institute of Solid State Physics, Russian Academy of Sciences, Chernogolovka, Russia

U. DAHMEN
National Center for Electron Microscopy, LBNL, Berkeley, CA, USA

Nanosized solid Pb inclusions in Al have fcc structure and perfect cuboctahedral shape. When the inclusions melt they attain a rounded equilibrium shape and due to the low miscibility between the two elements, the liquid inclusions are retained as individual nanosized droplets located inside the solid Al matrix. As the temperature is increased the smaller liquid Pb inclusions are observed to move in a three-dimensional random walk over distances that can be orders of magnitude larger than their size. Inclusions attached to dislocations exhibit a similar type of random walk confined to long-distance one-dimensional movement along the dislocation lines and short-range two-dimensional vibrations perpendicular to the dislocation lines. The diffusion coefficients of the moving inclusions can be obtained from an Einstein-Smoluchowski analysis of the inclusion traces providing input for information on the mechanisms responsible for the movements.

1. Introduction

The binary Al-Pb alloy system is monotectic with a large liquid miscibility gap and extremely low mutual solubilities in the solid phases [1]. When dilute alloys are made by rapid solidification through the miscibility gap the ribbons have a refined microstructure with nanosized pure Pb inclusions embedded in the pure Al matrix [2, 3].

The Pb inclusions have fcc structure and despite a lattice mismatch of 22% they grow in parallel cube alignment with the matrix. The shape of the inclusions is cuboctahedral bounded by {111} and {100} interfaces, and due to the high thermal vacancy activity in Al even at room temperature the inclusions impose no volume strain on the matrix [4]. These properties make the alloy extremely suited for in-situ heating experiments carried out in a transmission electron microscope (TEM). When thin TEM samples are heated to the melting point of the Pb inclusions where the Al matrix is still solid, the liquid Pb inclusions remain inside the Al matrix and both the melting transition and the behaviour of the liquid lead inclusions at even higher temperatures can be observed directly in the TEM and monitored using real-time video recording [5].

Melting of the inclusions is associated with a large size dependent superheating above the bulk melting point of 327°C that for the smallest inclusions, only a few nm in size, can reach values as high as 100°C [6]. When the inclusions melt they spontaneously change shape from a faceted to a rounded morphology, and although the complete shape change for the larger inclusions is kinetically limited, the final spherical equilibrium shape can eventually be reached by heating the inclusions to around 450–500°C [7]. Once the liquid Pb inclusions are rounded they are seen to move rapidly through the Al matrix over distances that are orders of magnitude larger than their size. The movement of free inclusions—inclusions that are not attached to pinning centers—resembles three-dimensional Brownian motion or random walk. Due to the absence of stress fields around the inclusions there are no mutual long-range interactions, and the random walks will continue until the inclusions reach the sample surfaces or coalesce with other inclusions [8]. Inclusions, on the other hand, that during the solidification process have become attached to dislocations will display rapid long-range one-dimensional random walk along the dislocation lines and small-scale random oscillations

*Author to whom all correspondence should be addressed.

perpendicular to the dislocation lines [9, 10]. In contrast to free inclusions that will coalesce when they accidentally meet, the inclusions that move along the dislocation line repel each other at close distances thus preventing coalescence.

In the present paper the one-dimensional random movement of four inclusions with different sizes attached to the same dislocation has been followed at 485°C by real-time video recordings. From digitized individual video frames the time trajectories of the inclusions have been analyzed in terms of the Einstein-Smoluchowski theory for random walks originally derived by Einstein for free particles [11] and later modified by Smoluchowski to include random motion in an attractive harmonic potential [12]. The dependence of the diffusion coefficients on inclusion size has finally been used to obtain information about the atomistic mechanisms that mediate the movement of the inclusions following the original analysis for movement of noble gas bubbles given by Nichols in 1969 [13] and Goodhew and Tyler [14].

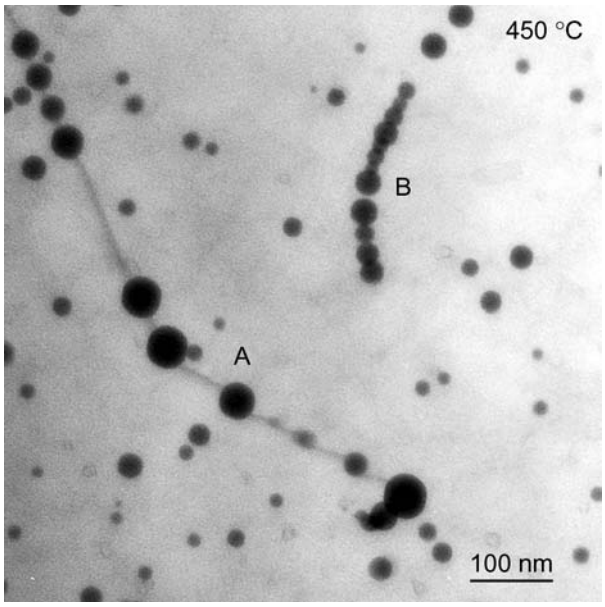

Figure 1 TEM micrograph taken at 450°C of liquid Pb inclusions embedded in Al. Many of the inclusions are attached to dislocations. At (A) the dislocation is visible while at (B) it is out of contrast.

2. Experimental

TEM samples of Al containing nanosized Pb particles were prepared from high-purity ribbons of Al with 0.65 at.% Pb obtained by rapid solidification from a temperature above the Al-Pb liquid miscibility gap. In-situ TEM studies of the movement of the inclusions were carried out at a temperature of 485°C in a 200 kV Philips CM 20 microscope using a Gatan single tilt heating stage. The observations were recorded on videotape (25 video frames per second). Trajectories of the inclusions projected into the plane of view were obtained from measurements of the positions of the centers of the Pb inclusions using a 30 s sequence containing 750 digitized images. The drift of the sample as a whole during the time of recording was ascertained from fixed points in the images.

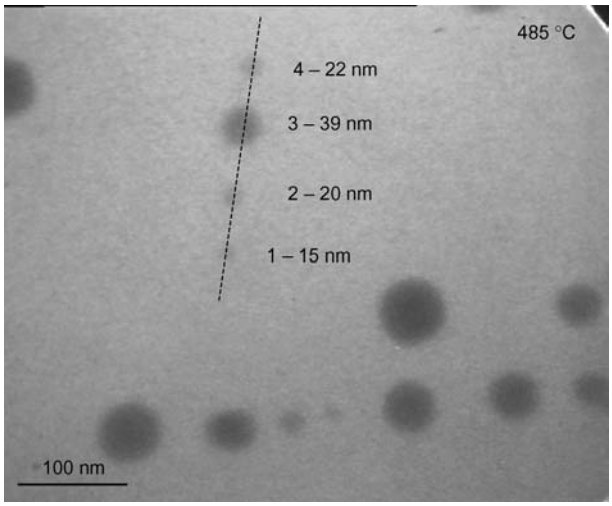

Figure 2 TEM micrograph at 485°C showing the four inclusions studied in the present work. The diameters of the four inclusions are: #1—15 nm, #2—20 nm, #3—39 nm, and #4—22 nm respectively. The inclusions are all attached to the same dislocation that is out of contrast. The image is the first frame from the video sequence used in the analysis with a duration of 30 s.

3. Results and discussion

Inclusions in the rapidly solidified Al-0.65 at.%Pb alloy typically have sizes in the range from about 10 nm to around 100 nm. Fig. 1 shows an example of such inclusions attached to a dislocation. The micrograph is taken at 450°C where all the inclusions are liquid but still display some tendency for retention of larger flat interface facets.

The set of inclusions used in the present study are shown in the TEM micrograph in Fig. 2. The four liquid lead inclusions labeled #1 to #4 have diameters of 15, 20, 22 and 39 nm respectively and they are attached to a dislocation that is out of contrast—the position of the dislocation is indicated by the dotted line. The micrograph is the first image of a video sequence with a duration of 30 s recorded at 485°C displaying vivid random movement of the inclusions in a direction parallel to the dislocation line. Movement of the inclusions as a function of time was obtained from the 750 individual video frames that were digitized and computer analyzed with a time resolution of 0.04 s corresponding to the video rate of 25 frames/s. Fig. 3a shows a section of the same image oriented with the dislocation line in vertical position and with an inserted X-coordinate indicating the direction of the position coordinates for the four inclusions in the movement parallel to the dislocation line. The random nature of the movement of the inclusions parallel to the dislocation line is clearly seen in the time traces (Fig. 3b) which also show that the average amplitude of the movement is size dependent—largest for the smallest inclusion (#1) and smallest for the largest inclusion (#3). Although the movement of the inclusions is random it is striking that coalescence of inclusions attached to the dislocations is very rarely seen while inclusions that move freely in the matrix coalesce when they accidentally meet.

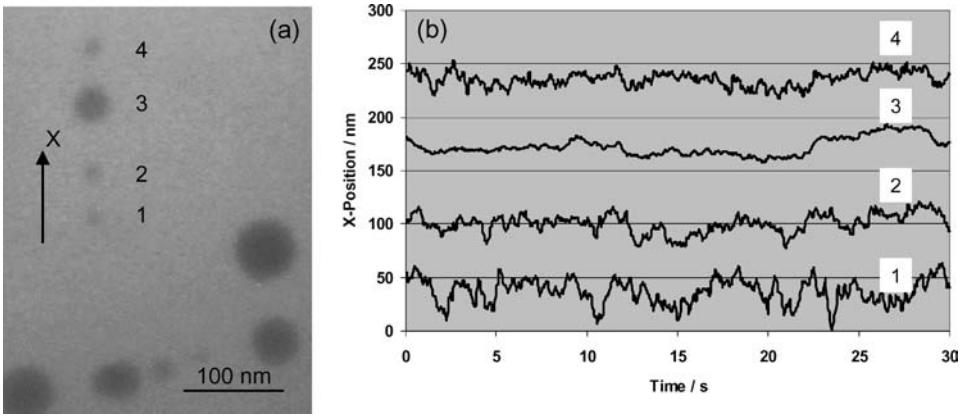

Figure 3 The four inclusions with the position coordinate X oriented vertically (a). Time traces for the four inclusions obtained from 750 consecutive video frames from a sequence with a duration of 30 s.

Analysis of random walks trajectories for motion of free unconstrained particles is carried out within the framework of diffusion theory using Einstein's relation for the mean square displacement $<\Delta x^2>$ of the particle as a function of time t [11]. For one-dimensional movement we have

$$<\Delta x^2>= 2Dt \tag{1}$$

where D is the diffusion coefficient. However, in the present experiment the movement of the inclusions is not free as the inclusions, due to the fact that they do not coalesce, are confined to remain in regions along the dislocation limited by the presence of the neighboring inclusions. Smoluchowski extended Einstein's analysis of free unconstrained random movement to cover the case of random movement of a particle in an attractive harmonic potential [12]. In this analysis the mean square displacement of the particle as a function of time is given by

$$<\Delta x^2> = 2\sigma_x^2\left\lfloor 1 - \exp\left(-Dt/\sigma_x^2\right)\right\rfloor \tag{2}$$

where σ_x is the is the average standard deviation of the particle from the origin of the potential. For small time steps this equation approaches the Einstein Equation 1 indicating that the particle movement resembles a free random walk, while for large times the average position of the particle will be a constant distance $\sqrt{2}\sigma_x$ from the origin.

From the time traces of the particles in Fig. 3b the mean square displacements $<\Delta x^2>$ along the dislocations for each particle have been obtained by running averages over the entire paths. The data have been plotted as a function of time (Fig. 4) for times up to 4 s, i.e. for 100 time steps. Each dataset was fitted to the Smoluchowski Equation 2 and the values obtained for the diffusion coefficients D and the average standard deviation of the particles σ_x are shown in Table I together with the values for the inclusion sizes. In the Einstein regime the data should fit to straight lines with slopes defining the values of the diffusion coefficients and in the Smoluchowski regime the 2nd axis intercepts will determine the σ_x values. The straight line fits in the Einstein regime are not as perfect as they would be for

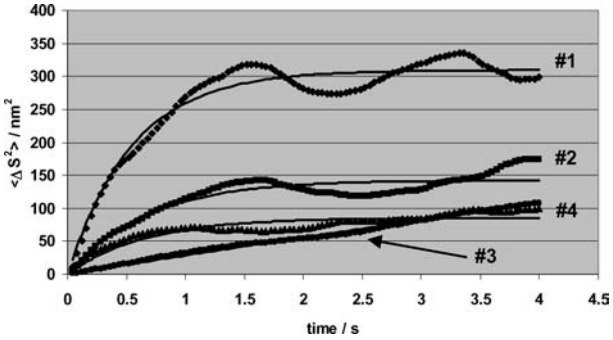

Figure 4 The mean square displacements as a function of time for the four inclusions displayed (data points) together with the functions fitted to Equation 2 (full lines) of the Einstein-Smoluchowski analysis. The fitted function to inclusions #3 is coinciding with the data points.

free unconstrained particles indicating that the Smoluchowski model is only a first order approximation for describing the complex movement of the inclusions. This is quite likely due to the fact that the inclusions, when they move randomly along the dislocations, are not always seeing the same repulsive potential from the neighboring inclusions but rather a potential that in a complex way will vary in strength and extent depending on the positions and velocities of the next nearest neighbors. This is also reflected in the behavior of the data in the transition zone from the Einstein to the Smoluchowski regime. Ideally, the transition should change smoothly from an inclined straight line at small times into a horizontal line for large t values, while the latter in most cases display some large-scale oscillations in the data. It is therefore not surprising that the dataset coming closest to ideal behavior is from the largest inclusion (#3) that moves the least and where the movement therefore also should be less sensitive to variations

TABLE I Sizes, diffusion coefficients and values for the mean displacements for the four inclusions in Fig. 2

Inclusion#	Size (nm)	D (nm^{2}s^{-1})	σ_x (nm)
1	15	282	12
2	20	107	9
3	39	17	–
4	22	66	7

in neighboring interactions. In Fig. 4 it can be seen that the mean square displacement for this inclusion is close to pure Einsteinian and the fit of the graph to Equation 2 therefore does not give a well-defined value for σ_x.

Using the dependence of the diffusion coefficient on inclusion size it is possible at a given temperature to obtain information on the mechanism that mediates the movement of the inclusions. The dependence of the diffusion coefficient D on the size d of the inclusions is often expressed by the relation

$$D = \frac{K_n}{d^n} \tag{3}$$

where n is an integer that is related to the mechanism causing the movement and K_n is a constant that depends on the given mechanism [13]. Equation 3, originally derived for diffusion of nanoscale noble gas bubbles in metals, is commonly used to distinguish between the following three mechanisms for $n = 2$, 3 or 4 respectively. For $n = 2$ movement of the inclusions is mediated by diffusion of matrix atoms moving through the volume of the inclusions, for $n = 3$ movement of the inclusions is caused by matrix vacancy migration caused by random variations in the matrix vacancy flux, and for $n = 4$ movement of the inclusions is caused by diffusion along the inclusion matrix interface. If, on the other hand, random movement of ledges in the inclusion matrix interface is responsible for the movement of the inclusions the dependence of the diffusion coefficient on the inclusion size is given by

$$D = k_1 d \cdot \exp(-k_2 d) \tag{4}$$

where k_1 and k_2 are constants [14].

In order to try to distinguish between the different mechanisms, the diffusion coefficients D obtained for the four inclusions (Table I) are plotted as a function of inclusion size d in a log-log plot (Fig. 5a) where a straight line fit gives a slope of -3.1, i.e. close to -3, which indicates that volume diffusion of matrix vacancies might be responsible for the movement of the inclusions. However, plotting ln (D/d) as a function of inclusion size d also fits fairly well to a straight line (Fig. 5b) indicating that movement of the inclusions mediated by a ledge mechanism expressed by Equation 4 might also be a possibility.

In an earlier work where the diffusion coefficient of free liquid Pb inclusions carrying out three-dimensional Brownian motion at 450°C was measured for different inclusion sizes, the size dependence was found to agree with a $1/d^4$ behavior indicating that the mechanism for movement of the inclusions might be controlled by interface diffusion [8]. In another experiments where the diffusion coefficient for a liquid Pb inclusion attached to a dislocation in the Al matrix was determined at ten temperatures in the region from 350–425°C it was found that the results displayed a two-stage Arrhenius behavior with a transition temperature around 375°C. The activation energy at the lower temperatures complied with a ledge or interface related mechanism while at higher temperatures it was in better accordance with a

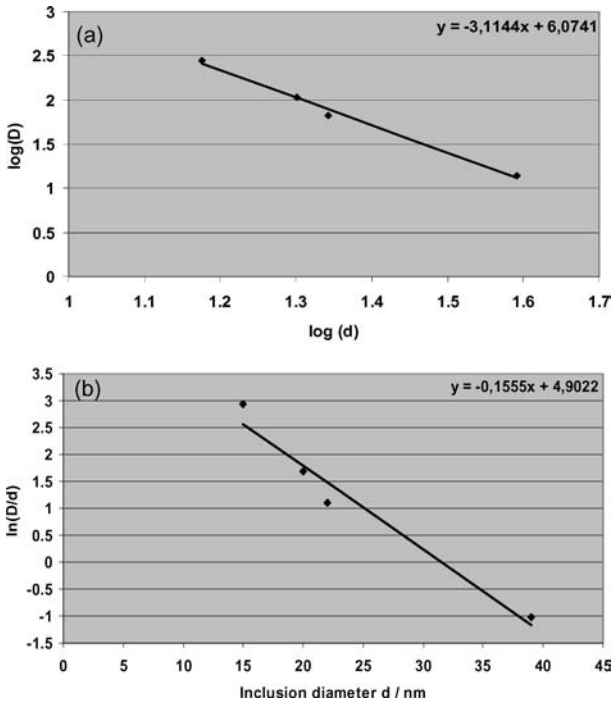

Figure 5 Log-log plot of the diffusion coefficient D of the four inclusions as a function of inclusion size d and a straight line fit with a slope of -3.1 (a). Plot of the diffusion coefficient of the four inclusions as a function of size—ln(D/d) vs d and a fit to Equation 4b (b).

volume vacancy diffusion mechanism [9]. The present experiment was carried out at the relatively high temperature of 485°C, i.e. above the top of the temperature range where the Arrhenius plot indicates that volume diffusion of matrix vacancies would control the movement of the inclusions. It is therefore consistent that the present analysis on the size dependence of the diffusion coefficients of the inclusions displays a $1/d^3$ behavior that also indicates volume vacancy diffusion control. However, this does not comply with the result obtained for free inclusions carrying out unconstrained movement. It is possible that the dislocation that tethers the inclusions also generates the necessary step in the interface to eliminate the nucleation barrier for motion along the dislocation line. In that case particle motion would no longer be controlled by step nucleation, and volume diffusion could become limiting. The precise role of the dislocation will depend on its characteristics such as the screw component and line direction. In order to make a full distinction between the different mechanisms, and in particular to see whether there is a fundamental difference between free inclusions and inclusions attached to dislocations, experiments with a larger number of inclusions with a bigger size spread and a more detailed analysis of the specific dislocation geometry are required.

4. Conclusions

Movements of nanosized liquid Pb inclusions in Al have been analyzed within the framework of random walks or Brownian motion. Inclusions attached to dislocations display long-range one-dimensional random walks along the dislocation lines and when several inclusions are attached to the same dislocation they move

in patterns that resemble a set of coupled random oscillators. Time series of video sequences recorded at 485°C have been used to determine the trajectories of four inclusions with different sizes attached to the same dislocation. Diffusion coefficients for the individual inclusions have been obtained from their time traces using an Einstein-Smoluchowski analysis valid for particles moving randomly in a harmonic potential. The size dependence of the diffusion coefficients indicates that movement of the inclusions at this particular temperature are mediated by volume matrix vacancies. However, experiments with a larger number of inclusions with a bigger size spread and a more detailed analysis of the character and role of the dislocation will be needed for an unambiguous assessment of the mechanism.

Acknowledgements

This work was supported by the Danish Natural Sciences Research Council and the Director, Office of Science, Office of Basic Energy Sciences, Division of Materials Sciences and Engineering, of the U.S. Department of Energy under Contract No. DE-AC03-76SF00098. We are grateful to P. Ochin for supplying the melt–spun alloys.

References

1. C. J. SMITHELLS and E. A. BRANDES (eds.), in "Metal Reference Book" (Butterworths, Boston, 1976).
2. K. I. MOORE, K. CHATTOPADHYAY and B. CANTOR *Proc. Roy Soc. Lond.* **A414** (1987) 499.
3. K. I. MOORE, D. L. ZHANG and B. CANTOR, *Acta Metall. Mater.* **38** (1990) 1327.
4. E. JOHNSON, A. JOHANSEN, U. DAHMEN, S. CHEN and T. FUJII, *Mater. Sci. Eng.* **A304–306** (2001) 187.
5. H. H. ANDERSEN and E. JOHNSON, *Nucl. Instrum. Meth.* **B106** (1995) 480.
6. L. GRÅBÆK, J. BOHR, H. H. ANDERSEN, A. JOHANSEN, E. JOHNSON, L. SARHOLT-KRISTENSEN and I. K. ROBINSON, *Phys. Rev. B* **45** (1992) 2628.
7. H. GABRISCH, L. KJELDGAARD, E. JOHNSON and U. DAHMEN, *Acta. Mater.* **49** (2001) 4259.
8. S. PROKOFIEV, V. ZHILIN, E. JOHNSON, M. LEVINSEN, J. S. ANDERSEN, U. DAHMEN, T. RADETIC and J. TURNER, in Proc. VIII Seminar on Diffusion and Thermodynamics of Materials, edited by J. Cermak and J. Vrest'al (Brno, Czech Republic, 2002) p. 241.
9. E. JOHNSON, J. S. ANDERSEN, M. LEVINSEN, S. STEENSTRUP, S. PROKOFJEV, V. ZHILIN, U. DAHMEN, T. RADETIC and J. H. TURNER, *Mater. Sci. Eng.* **A375–377** (2004) 951.
10. E. JOHNSON, M. T. LEVINSEN, S. STEENSTRUP, S. PROKOFJEV, V. ZHILIN, U. DAHMEN and T. RADETIC, *Philos. Mag.* **84** (2004) 2663.
11. A. EINSTEIN, *Ann. d. Phys.* **17** (1905) 549.
12. M. V. SMOLUCHOWSKI, Bull. Int. de l'Acad. de Cracovie, Classe de Sci. Math. et Nat. Serie **A** (1913) 418.
13. F. A. NICHOLS, *J. Nucl. Mater.* **30** (1969) 143.
14. P. J. GOODHEW and S. K. TYLER, *Proc. Roy. Soc.* **377** (1981) 151.

Received 17 September 2004
and accepted 31 January 2005